

Random packings of spiky particles: Geometry and transport properties

I. Malinouskaya^{a,b}, V.V. Mourzenko^b, J.-F. Thovert^b, P.M. Adler^a

a. Institut P', Département Fluides, Thermique, Combustion, ENSMA - 1, av. Clément Ader - BP 40109, 86961 Futuroscope Cedex

b. UPMC Sisyphe, BP 105, 4 Place Jussieu, 75252 Paris Cedex 05

Résumé :

Des particules hérissées sont construites par superposition de sphères et d'ellipsoïdes allongés. Des empilements aléatoires de ces particules sont obtenus en simulant une déposition séquentielle. La géométrie, la conductivité et la perméabilité des empilements sont analysés de manière systématique en relation avec les caractéristiques des grains. On propose des corrélations générales reliant ces propriétés à l'indice de sphéricité et à une taille équivalente de grain.

Abstract :

Spiky particles are constructed by superposing spheres and prolate ellipsoids. The resulting nonconvex star particles are randomly packed by a sequential deposition algorithm. The geometry, the conductivity, and the permeability of the resulting packings are systematically studied, in relation with the individual grain characteristics. Overall correlations are proposed to approximate these properties as functions of the grain equivalent size and sphericity index.

Mots clefs : Granular media, conductivity, permeability

1 Introduction

Random packings of grains can be found in various natural environments as well as in industrial applications and they are a very interesting topic for scientific research due to their very complex behaviour. Most earlier works were devoted to random packings of spheres, whether they are mono or polydisperse and the studies devoted to nonspherical particles are much less common and are mostly experimental. A review of the recent works is given in [1].

The purpose of this paper is to study the packings of star particles which are not convex. Each grain is obtained by addition to a sphere of one or more identical ellipsoids with the same center. Because of their general aspect, these particles are called spiky. Since they are yet nearly unexplored, there is a fundamental interest in the study of the properties of non convex grain packings. In addition, the kind of particles considered here is reminiscent of various objects such as grafted particles, some pellets, flakes or small grain clusters. Therefore, the present results can find applications in a variety of industrial situations.

The generation of the spiky particles, the various shapes which were studied and the sequential algorithm which is used are described first. The geometrical properties of the particles such as the volume, the surface and the sphericity index are presented. Collective properties of the packings are also studied, namely porosity, hydraulic radius, correlation functions and orientation.

Then, transport properties are studied. The macroscopic conductivity is derived by solving the Laplace equation. Permeability is obtained by solving the Stokes equations.

All the technical details about this work can be found in [1], where additional results are also provided.

2 Random packings of different types of grains

Since packings of spherical and ellipsoidal particles are easily generated, the new grain shapes are based on these forms. Therefore, all the particles are composed by a sphere and each new form of grain is obtained by addition to this sphere of one or more identical ellipsoids with the same center. The positions of the ellipsoids are chosen in order to produce grains which are relatively regular and isotropic. However, two anisotropic types of grains are also considered.

The grains are defined by the distance R between a point $\mathbf{X}_G(X_G, Y_G, Z_G)$ called the center and its surface. Often \mathbf{X}_G is the center of gravity of the particle. Let us consider each particle in its local coordinates with the origin at \mathbf{X}_G . This distance R is determined in the polar coordinates for each orientation (Θ, ϕ) ; Θ is the inclination with respect to the z -axis and ϕ is the rotation of the x -axis around the z -axis (Fig.1a). Then, the surface of the particle is represented as

$$r = R(\Theta, \phi) \quad (1)$$

For a spherical grain, the function $R(\Theta, \phi)$ is simply equal to the radius of the sphere R_{sph} . For an ellipsoidal grain with semiaxes (R_x, R_y, R_z) aligned with the axes of coordinates, it can be written as

$$R_{ell}(\Theta, \phi) = \left\{ \frac{\cos^2(\Theta)}{R_z^2} + \sin^2(\Theta) \left[\frac{\cos^2(\phi)}{R_x^2} + \frac{\sin^2(\phi)}{R_y^2} \right] \right\}^{-1/2} \quad (2)$$

In all cases, the two semiaxes R_x and R_y of each ellipsoid are identical and smaller than R_z . Therefore, the position of the ellipsoid is fully determined by the orientation of its major axis.

Since all the grains are made of one sphere and N_{ell} ellipsoids, the corresponding functions $R(\Theta, \phi)$ are expressed in terms of R_{sph} and $R_{ell}(\Theta, \phi)$. More precisely, $R(\Theta, \phi)$ can be expressed as

$$R(\Theta, \phi) = \max \left\{ R_{sph}, R_{ell}^{(j)}(\Theta, \phi) \right\}, \quad j = 1, \dots, N_{ell} \quad (3)$$

Examples of such particles are given in Figs.1b-h. There are two types of anisotropic grains. The first one, called one-ellipsoid, is the particle obtained by the addition of one sphere and one ellipsoid (Fig.1b). The second one, called two-ellipsoid, is the addition of one sphere and two ellipsoids (Fig.1c).

The regular polyhedra Ph (tetrahedron, cube, octahedron, dodecahedron and icosahedron) were used as a basis for the regular particles. The center of the grain sphere is the center of the polyhedron circumsphere. The ellipsoids are oriented orthogonally to the faces of Ph (Fig.1d-h). Hence, each ellipsoid generally corresponds to two faces with opposite normals.

Since the basis of all types of grains is a sphere of radius R_{sph} , let R_{sph} be the length unit, *i.e.*, for the numerical simulations $R_{sph} = 1$. Then, R_1 , R_2 and R_3 denote the ellipsoid semiaxes normalized by R_{sph} . Moreover, R_3 is defined as the major semiaxis and R_{12} as the minor ones

$$R_3 > R_{1,2} = R_1 = R_2 \quad (4)$$

The random packings result from the successive deposition of grains in "gravitational" field as follows [1, 2]. The grains are introduced at a random location above the bed already in place and fall until they reach a local minimum of their potential energy. During their fall, any displacement and rotation that contribute to lower their barycenter are allowed. The grains are deposited in a square vertical box, with a flat bottom at $z = 0$, and periodicity conditions along the x and y directions in order to avoid the well-known hard wall effects. This means that a particle may sit astride the border between two adjacent cells and interact with the rest of the packing on either side.

The box dimensions are set according to the major particle radius : $10 \times 10 \times 60 R_3^3$ (Fig.1i). The $10R_3$ top and bottom layers are discarded. This yields $10 \times 10 \times 40 R_3^3$ samples which are used for all the geometrical and transport property determinations. They contain from 1000 to more than 20000 grains, depending on their shape. Small parts of such samples are shown in Figs.1j-l.

For the solution of the transport problems and of some geometrical parameters (*e.g.*, R_H), the packing geometry was discretized into cubic volume elements of size a^3 , with as a rule $a = 1/4$. However, calculations were also done with $a=1/8$, $1/12$ and $1/16$ in a variety of typical situations. Corrective formulas for the discretization effects were established and systematically applied to the results.

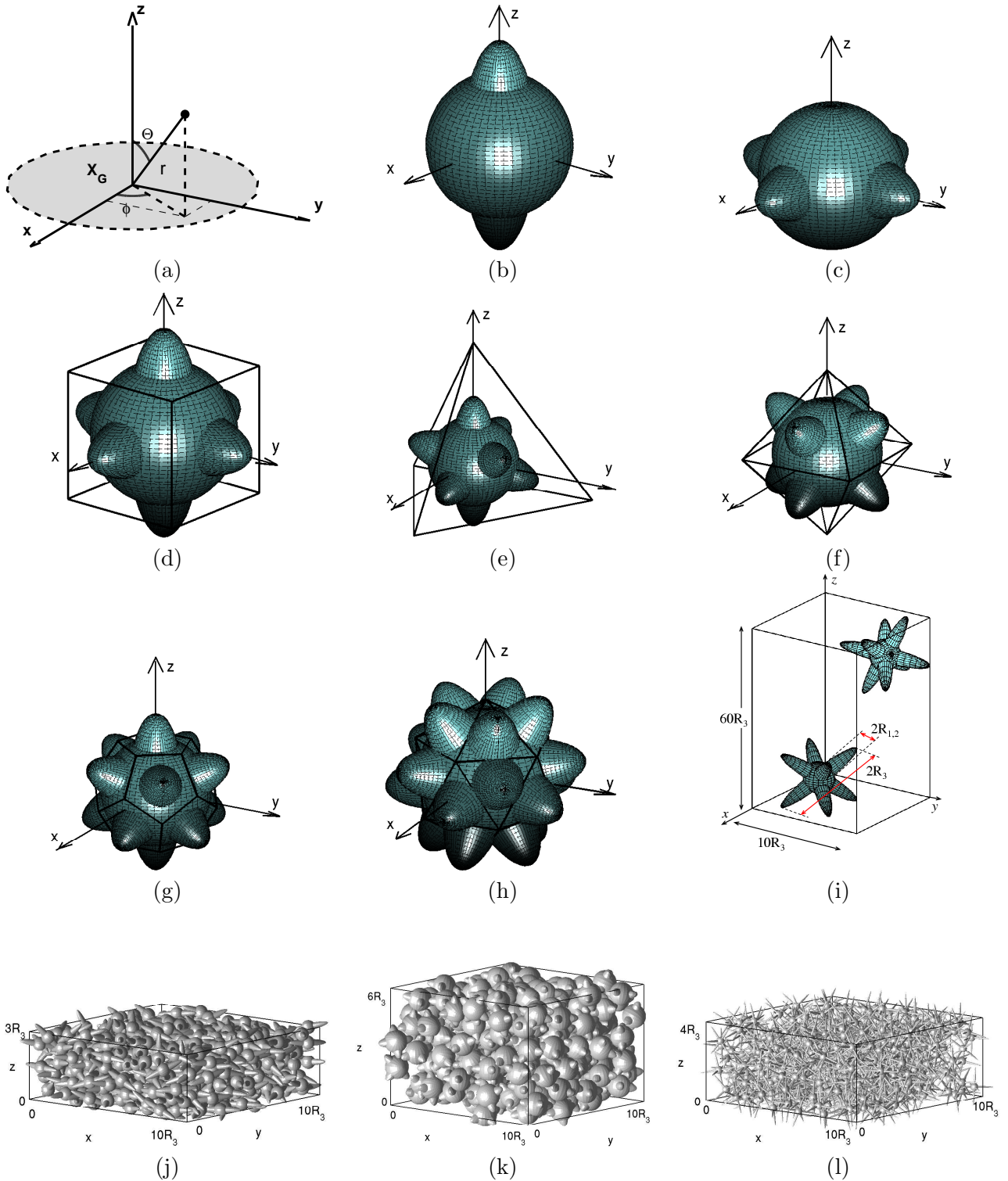


FIGURE 1 – (a) The particle definition in the polar coordinates (Θ, ϕ). Non regular particles : (b) one-ellipsoid particle ; (c) two-ellipsoid particle. Regular particles : (d) C-shaped (cube) ; (e) T-shaped (two tetrahedra) ; (f) O-shaped (octahedron) ; (g) D-shaped (dodecahedron) ; (h) I-shaped (icosahedron). Sketch of the unit cell with periodic boundary conditions and illustration of some geometrical notations (i). Parts of some numerical packing samples : One-ellipsoidal particles, $R_{1,2}=0.5, R_3=3$ (j) ; Two-ellipsoidal particles, $R_{1,2}=0.5, R_3=1.5$ (k) ; C-shaped particles, $R_{1,2}=0.25, R_3=5$ (l).

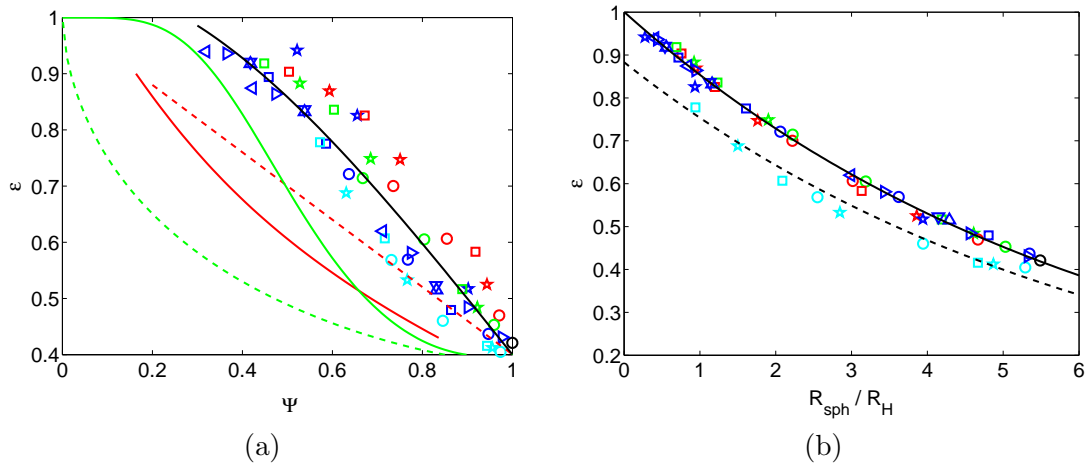


FIGURE 2 – (a) Porosity as a function of Ψ . The black solid line corresponds to (6). The red solid and broken lines are the empirical correlations of [3, 4] and the green lines are the envelop of the data of [5], for convex aspherical grain packings. (b) The porosity ϵ as a function of R_{sph}/R_H ; the solid and dashed lines correspond to (7) and (8), respectively. The colors correspond to the value of the ellipsoid semiminor axis : $R_{1,2}=0.15$ (red), 0.25 (green), 0.50 (blue), and 1.00 (cyan). The symbol shapes indicate the type of grain : one-ellipsoid (\circ), two-ellipsoid (\star), C-shaped (\square), O-shaped (∇) T-shaped (\triangle), D-shaped (\triangleright) and I-shaped (\triangleleft). The black circle corresponds to spherical particles. Identical symbols correspond to $R_3=1.5, 3$ or 5 , in decreasing Ψ order.

3 Geometric properties

In order to examine the influence of the type of grains on the packing geometrical and transport properties, some single particle characteristics, such as their volume V_1 , surface area S_1 and sphericity index Ψ have to be determined first. The radius R_v of the equivalent sphere is deduced from V_1 , and Ψ is defined as the ratio between the equivalent sphere surface S_v and the particle surface S_1

$$R_v = \left(\frac{3V_1}{4\pi} \right)^{1/3}, \quad \Psi = \frac{S_v}{S_1} \quad (5)$$

Several models are compared in [1] for the porosity as a function of R_v and Ψ . The following one does not make any reference to the detail of the grain shape and provides a fair prediction of the bed porosity, within about ± 0.1 (Fig.2a)

$$\epsilon = 0.40 + (1 - \Psi) + (1 - \Psi)^3 / 3 \quad (6)$$

For comparison, the empirical correlations of [3, 4] and the envelop of the data of [5] are also shown in Fig.2a. They correspond to grains with various aspherical but convex shapes. Clearly, the present non convex particles yield much larger porosities than convex particles with an identical Ψ .

The correlation between the porosity ϵ and the hydraulic radius R_H (ratio of the pore volume to the pore surface area) is examined in Fig.2b for all types of grains. All the data for particles with $R_{1,2} < 1$ are gathered and the porosity depends on the hydraulic radius as follows

$$\epsilon = \exp \left(-0.159 \frac{R_{sph}}{R_H} \right) \quad (7)$$

Note that the rightmost point corresponds to a sphere packing. All other particle shapes yield a larger hydraulic radius and a larger porosity. The results for particles with $R_{1,2} = 1$ are gathered into another group. For $R_{sph}/R_H \leq 4$, they are well represented by the introduction of a prefactor in (7)

$$\epsilon = 0.88 \exp \left(-0.159 \frac{R_{sph}}{R_H} \right) \quad (8)$$

4 Transport properties of the packings

The macroscopic conductivity and permeability were deduced by integrating the local fields obtained by solving the Laplace and Stokes equations, respectively, on the pore scale, with a prescribed macroscopic potential or pressure gradient [1, 2, 6]. The solution is performed by using a finite volume formulation of the problems, in the cubic discretization of the packing geometry.

Note that periodicity conditions have been applied along the x -, y - and z -axes when computing the transport properties. The packing are indeed periodic along x and y , but not along z . Since the computation domains are typically 4 to 5 times higher than wide, this has only a marginal influence on the results.

4.1 Conductivity

Electrical and thermal conductions are governed by a Laplace equation

$$\nabla^2 T = 0 \text{ with } \mathbf{n} \cdot \nabla T = 0 \text{ on } S_p \quad (9)$$

where T is the local field, S_p is the solid insulating wall and \mathbf{n} its unit normal.

The temperature gradient ∇T is spatially periodic. In addition, either the average temperature gradient $\overline{\nabla T}$ or the average heat flux $\overline{\mathbf{q}}$ is specified. It is related to the average temperature gradient $\overline{\nabla T}$ by the symmetric positive definite conductivity tensor σ which depends only upon the geometry of the medium

$$\overline{\mathbf{q}} = -\sigma \cdot \overline{\nabla T} \quad (10)$$

The calculations of the conductivity tensor σ were performed for the packings described above. The effects of the anisotropy and discretization were studied. The average over all directions $\bar{\sigma}$ is used and it was extrapolated for infinitely small discretization σ_∞ . The results are described by Archie's law (11) and shown in Fig.3a

$$\sigma_\infty = 0.98\epsilon^{1.422} \quad (11)$$

4.2 Permeability

Permeability can be derived from the solution of Stokes equation

$$\nabla p = \mu \nabla^2 \mathbf{v}, \quad \nabla \cdot \mathbf{v} = 0 \text{ with } \mathbf{v} = 0 \text{ on } S_p \quad (12)$$

where \mathbf{v} , p and μ are the velocity, pressure and viscosity of the fluid, respectively.

The macroscopic pressure gradient $\overline{\nabla p}$ is related to $\overline{\mathbf{v}}$ by the permeability tensor \mathbf{K}

$$\overline{\mathbf{v}} = -\frac{1}{\mu} \mathbf{K} \cdot \overline{\nabla p} \quad (13)$$

\mathbf{K} is a symmetric positive definite tensor. Similarly to the conductivity tensor σ , \mathbf{K} takes the same values along x - and y -axes and can be slightly different along z .

There are several classical models to represent the dependence of the permeability on the geometric packing characteristics. For example, the normalization of the permeability \mathbf{K} by the square of the equivalent sphere radius R_v^2 was successively used by [2] to gather the results for packings of spheres, ellipsoids and parallelepipeds. The most classical model is the Carman-Kozeny equation

$$K = \frac{\epsilon R_H^2}{k} \quad (14)$$

where k is the Kozeny constant.

In order to reduce the numerical errors attached to the results of calculations with a finite discretization step, extrapolated values are used [1]. The anisotropy appears to be negligible and a global numerical fit can be found as

$$\frac{k_\infty}{\Psi^2} = \frac{3.20}{1 - \epsilon} \quad (15)$$

The ratio k_∞/Ψ^2 is plotted in Fig.3b as a function of porosity.

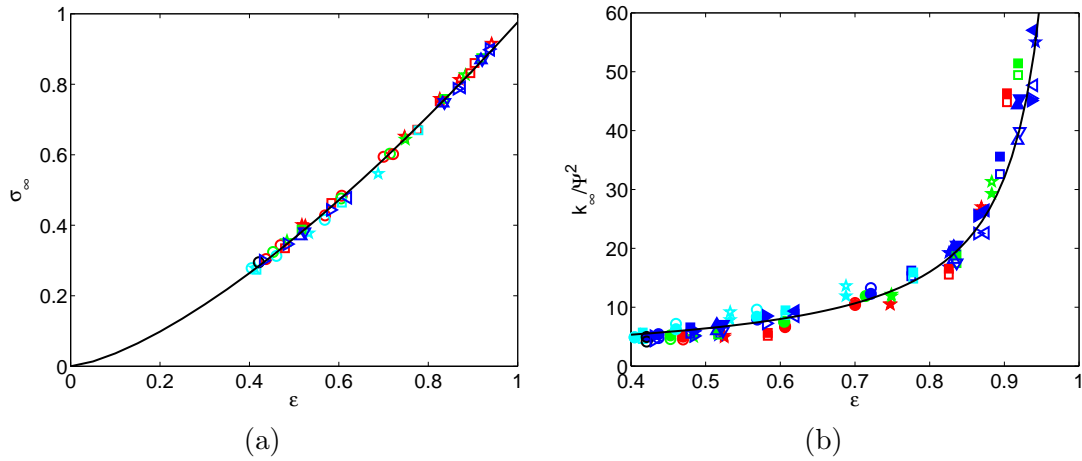


FIGURE 3 – (a) The extrapolated conductivity σ_∞ as a function of porosity; the line corresponds to the fit (11). (b) The ratios $k_{x,\infty}/\Psi^2$ and $k_{z,\infty}/\Psi^2$ as functions of ϵ ; the solid line is the numerical fit (15). The data are the calculated transport coefficients as functions of the porosity measured in the same samples. Same conventions as in Fig.2 for the symbol colors and shapes. The conductivities in (a) are averages over the x -, y - and z -directions. The Kozeny constants in (b) are calculated along the z -direction (open symbols), or averaged over the x - and y -directions (close symbols).

5 Conclusions

Packings of complex particles have been generated. Then, their geometric and transport properties were numerically calculated and their dependence on the single grain characteristics has been studied. The influence of the anisotropy and discretization effects were taken into account.

The most important geometrical characteristics of any porous medium is the porosity ϵ . It was shown to be a function of the sphericity index Ψ , as given by the numerical fits (6-8). The particles investigated here yield much larger porosities than convex particles with an identical sphericity index.

The hydraulic radius R_H can be deduced from Ψ by taking (6) into account.

Similarly, the transport properties, such as the conductivity and the permeability, can be expressed in terms of the sphericity index and of the equivalent sphere radius. Archie's law applies and the conductivity σ is a function of the porosity given by (11). The permeability can be determined in terms of the Kozeny constant k which can be predicted by (15).

Références

- [1] Malinouskaya, I., Mourzenko, V.V., Thovert, J.-F., Adler, P.M., Random packings of spiky particles : Geometry and transport properties, *Phys. Rev. E*, **80**, 011304 (2009).
- [2] Coelho D., Thovert J.-F. and Adler P.M., Geometrical and transport properties of random packings of spheres and aspherical particles, *Phys. Rev. E*, **55**, 1959-1978 (1997).
- [3] Warren J. and R. M. German, in *Modern Developments in Powder Metallurgy*, edited by P. M. Gummeson and D. A. Gustatson (Metal Powder Industries Federation, New Jersey, 1988), Vol. 18, pp. 391-402.
- [4] Thies-Weesie D. M. E., A. P. Philipse and S. G. I. M. Kluijtmans, Preparation of sterically stabilized silica-hematite ellipsoids : Sedimentation, permeation, and packing properties of prolate colloids, *J. Colloid Interface Sci.*, **174**, 211-223 (1995).
- [5] Zou R. P. and A. B. Yu, Evaluation of the packing characteristics of monosized nonspherical particles, *Powder Technol.*, **88**, 71-79 (1996).
- [6] Adler P.M., *Porous Media : Geometry and Transports* (Butterworth/ Heinemann, Stoneham, MA, 1992).